

Computer Modeling of Hailstone Growth in Feeder Clouds

DENNIS J. MUSIL

Institute of Atmospheric Sciences, South Dakota School of Mines and Technology, Rapid City

(Manuscript received 29 December 1969)

ABSTRACT

The growth of hailstones is studied using a one-dimensional non-steady-state model of a growing feeder cloud. Conditions within the mature cloud are assumed to be adiabatic. Vertical velocity and liquid water content profiles change at a predetermined rate, beginning with small values and gradually increasing to values that can be expected in a mature thunderstorm.

Hailstone growth equations used in the model are developed in terms of the well-known dry- and wet-growth regimes and include terms that account for growth in a mixture of supercooled cloud droplets and ice crystals. Hailstone embryos in the form of liquid cloud droplets are introduced into the model at various heights and times, and the subsequent trajectories are analyzed. Different versions of the model that incorporate changes in updraft magnitude and shape are tested.

Results show that the model produces hailstones, radii ranging from near zero to 1.3 cm in 40 min or less, from 20 to 50 μ radius embryos introduced under a variety of updraft conditions, at many places in the life of the feeder cloud model.

1. Introduction

Feeder clouds are one of the most striking visual phenomena associated with Great Plains hailstorms. They form as small cumulus clouds, sometimes arranged in lines, at distances up to 20 mi away from the hailstorm core. Each feeder cloud grows rapidly as it approaches and merges with the main cumulonimbus cloud mass. Merger usually takes place at the southwest side of the main cloud mass and occurs 15–40 min after the formation of the feeder cloud. A first radar echo usually appears in a feeder cloud just before it merges with the main cloud mass and the merger is often followed by an upsurge of storm activity with a burst of heavy rain or hail at the ground (Dennis *et al.*, 1970).

Elementary reasoning suggests that feeder clouds are a favored region for hail formation, because the evolving hydrometeors within them are not subjected to extremely strong updrafts until some time after the initial cloud formation. This reduces the tendency noted in steady-state numerical models for reasonably sized hailstone embryos to be carried above the supercooled portions of the cloud before reaching appreciable size. Because both observations and this line of reasoning suggest an important role for feeder clouds in hail formation, the growth of hailstones within them has been studied with the aid of a simple numerical model. The numerical model devised and the results of the computations are given in the following sections.

2. The model

a. Background

The model resembles that developed by Hitschfeld and Douglas (1961) to study Alberta hailstorms

(Douglas, 1963) in that it is one-dimensional and emphasizes hailstone growth around embryos¹ of 20–50 μ as a function of temperature and cloud water content. It differs in being time-dependent, a necessary feature for a feeder cloud model.

b. Hailstone embryos

The question of the origin and size of the hailstone embryos is basic to the development of a hailstone growth model. One source might be the large liquid cloud droplets, which freeze while being carried aloft in the clouds, and thus become the hailstone embryos (Humphreys, 1940). Ludlam (1958) proposed that the embryos likely are rare large cloud droplets occurring near the bases of clouds.

Despite measurements made by various authors (e.g., Weickmann and aufm Kampe, 1953; Battan and Reitan, 1957), which have shown most cloud droplets to be very small, there is ample evidence of the existence of large cloud droplets, especially near the bases of cumulus clouds. Ludlam (1959) found 20 μ droplets near the bases of cumulus clouds in concentrations of 20 m^{-3} . MacCready and Takeuchi (1968) found similar concentrations of droplets as large as 30 μ below the cloud base. These grew by coalescence to even larger sizes within the cloud. Kopcewicz (1965), reporting on work done by the Russians, reports droplet concentrations on the order of 1 m^{-3} in the 20–50 μ size range near the bases of developing cumulus clouds. Furthermore, Rosinski and Kerrigan (1969) have made measurements of large water-insoluble aerosol particles (>35–40 μ)

¹ Unless otherwise specified, size will be defined as the radius throughout this paper.

around which droplets can form, and suggest that these play a role in the formation of rain and hail in severe thunderstorms.

In line with these recent measurements, liquid cloud droplets with radii from 20–50 μ are used as hailstone embryos in this study. The embryos are arbitrarily assumed to freeze at an in-cloud temperature of -15°C .

c. Hail growth equations

One of the first considerations in the development of a hailstone growth model must be the equations that describe the growth of a hailstone in a given cloud environment. They are derived most conveniently in terms of the heat balance. It is well known (e.g., Ludlam, 1958) that hailstone growth can be dry or wet. In dry growth, the temperature of the stone is below 0°C and all the cloud water intercepted by the stone is frozen to it. In wet growth, the surface of the stone is at 0°C and the heat added to the hailstone during the freezing process cannot be transferred to the surroundings fast enough to permit all the cloud water intercepted by the stone to be collected.

The equations describing the growth of hailstones in a mixed liquid/solid environment under conditions of dry and wet growth are derived and discussed in the Appendix. Critical parameters in the equations related to the hailstones themselves are terminal velocity, collection efficiency and hailstone density.

Experimentally determined terminal velocities are used (Byers, 1965; Gunn and Kinzer, 1949; Macklin and Ludlam, 1961). As these values apply near sea level, a correction factor amounting to an increase of 4% km^{-1} was used (Atlas, 1966) to account for the effect of decreasing air density with altitude.

The collection efficiency E_i for liquid cloud droplets is taken to vary linearly from 0.5–1.0 for embryos increasing from 20–45 μ and is considered to be 1.0 for all embryos $>45 \mu$ (Atlas, 1966). The collection efficiency E_s for solid (ice) cloud particles is set at 0.25 for dry growth (Saunders, 1968) and at 1.0 for wet growth regardless of embryo size. The growth of a hailstone depends upon the availability of both liquid droplets and ice crystals.

It is beyond the scope of this paper to isolate the effects of density changes upon growth rate. Therefore, the density ρ_e of the rime deposited on the hailstone is set at a constant value of 0.9 gm cm^{-3} . This value is greater than the 0.3 gm cm^{-3} assumed by Ludlam (1958) and the 0.7 gm cm^{-3} assumed by Das (1962), but agrees with observations by Vittori and Caporai (1959).

3. Specifications of cloud conditions

a. Temperature, pressure and mixing ratio profiles

Vertical profiles of temperature, pressure and mixing ratio were obtained from the 1200 GMT Rapid City radiosonde for 17 July 1968, a day that produced

extensive hail in the area. For cloud temperatures, moist adiabatic conditions were assumed.

Using these profiles, many of the parameters in the hail growth equations can be found using analytic expressions as outlined in the Appendix. Thermal conductivity and viscosity are functions of temperature alone, while diffusivity is a function of both temperature and pressure. In order to find the Reynolds number, the air density must be known, which in turn requires pressure and virtual temperature. The virtual temperature can be computed when the mixing ratio is known. Once the Reynolds number is known, the ventilation coefficient can be computed. Saturation vapor density, which is also a function of temperature, is available from the *Smithsonian Meteorological Tables* (List, 1958), hereinafter referred to as the *Smithsonian Tables*.

b. Liquid water content profiles

Measurements of liquid water content in cumulus clouds are quite numerous, especially for the early stages of development. Liquid water contents in cumulus clouds are generally found to be less than moist adiabatic (e.g., Warner, 1955; Draginis, 1958; Hirsch and Schock, 1968). Estimates of very high liquid water contents in cumulonimbus clouds have been made by various authors (Donaldson, 1961; Kopcewicz, 1965); however, these are based on radar returns and are subject to uncertainties.

In view of the uncertainty involved, it was decided to use adiabatic values of liquid cloud water for the mature clouds, which probably holds true in the core region at least. Since there appears to be some relationship between cloud water and the stages of the cloud's development, i.e., smaller clouds having significantly less than adiabatic values, an arbitrary percentage of adiabatic liquid water content was used in the earlier stages of the life cycle of the cloud.

Profiles of liquid water content at 4-min intervals over a 28-min period are shown in Fig. 1. The moist adiabatic values were obtained from the 1200 GMT Rapid City radiosonde for 17 July 1968. Moist adiabatic values are used in the 20-, 24- and 28-min profiles, while the five earlier profiles use values increasing from 50–90% of the adiabatic value.

The model accounts for mixtures of liquid and ice. It is assumed that the freezing process begins at -20°C and that the cloud water is completely frozen at -40°C . Fig. 2 shows the percent of cloud water assumed to be frozen as a function of temperature. The freezing process begins slowly and the rate increases as the temperature decreases (Vali and Stansbury, 1965).

c. Updraft profiles

The specification of time-dependent updrafts was based on a combination of measurements (Sulakvelidze *et al.*, 1967) and results of a computer cloud model (Weinstein and Davis, 1968; Davis *et al.*, 1969).

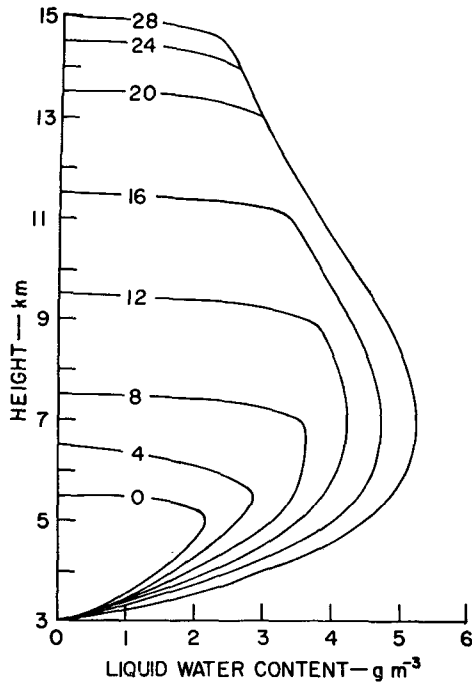


FIG. 1. Liquid water content profiles used in the feeder cloud model. Profiles are given in 4-min time intervals. Moist adiabatic values were obtained for the 28-min profile using the 1200 GMT Rapid City radiosonde of 17 July 1968. The cloud base was assumed to be at 3 km.

An example of one set of updraft profiles is shown in Fig. 3. The number on each profile represents the time in minutes at which each profile applies. The maximum was set at a height corresponding to 75% of each cloud's thickness, and the base² of the cloud was arbitrarily set at 3 km. The profiles labeled 20, 24 and 28 are identical below the maximum because the feeder cloud is approaching a mature state.

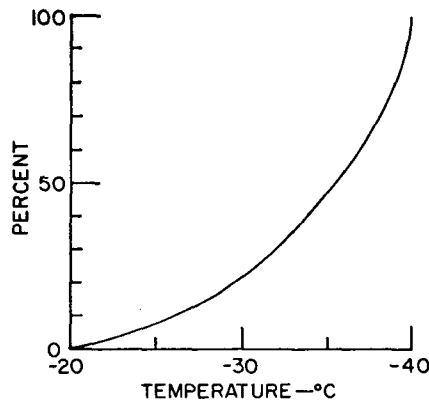


FIG. 2. Assumed percentage of frozen cloud water as a function of in-cloud temperature. Freezing was assumed to occur between -20 to -40°C in this model.

² Heights are considered with respect to mean sea level throughout this paper.

One of the items to be investigated in this model is the effect of changing updraft shape and intensity, with other conditions remaining unchanged. Since this requires various sets of updraft profiles, it is convenient to specify different versions of the feeder cloud model. The code consists of a letter representing the shape of the updraft profile, followed by a two-digit number that refers to the strongest vertical velocity in the series of profiles. As the shape of the updraft profiles shown in Fig. 3 is roughly similar to those obtained from the Penn State model (Weinstein and Davis, 1968), this version of the model is designated P25. Other versions that use the same shape profiles have been generated by reducing the magnitude of each updraft profile given in Fig. 3 by a factor of 2 and by increasing each profile by a factor of 1.5. These versions are called P12 and P37, respectively. Still another version was obtained by setting the updraft maximum at the midpoint of the cloud. This is in agreement with Russian measurements (Sulakvelidze *et al.*, 1967), and hence has been designated R25.

In all versions, the rate of rise of the cloud top is set initially at approximately one-half of the maximum vertical velocity, in agreement with the bubble theory of convection (Scorer, 1958). As the cloud matures, the rate is slowed considerably. The fact that updrafts exceed rate of rise of the cloud top causes some particles to be carried to the very top of the rising cloud. Any particle which comes within 200 m of the cloud top is assumed to be ejected from the updraft.

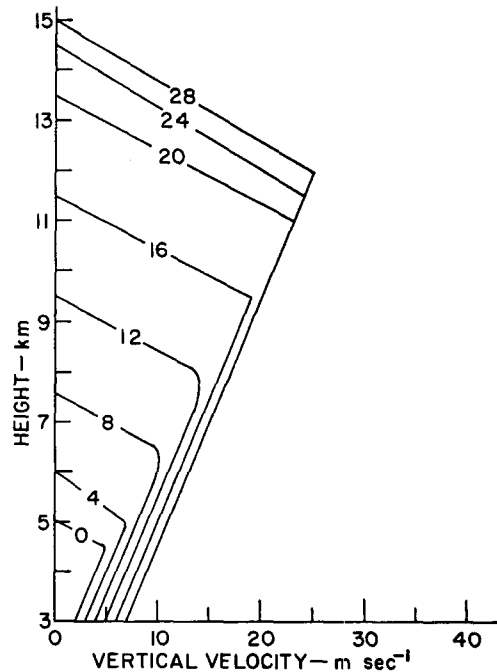


FIG. 3. Example of vertical velocity profiles used in the feeder cloud model. Profiles are given in 4-min time intervals. The maxima are placed at 75% of each profile's thickness.

4. Computer program

A computer program was written incorporating Eqs. (A6) and (A10)—see Appendix.

Many of the items discussed in Section 3 were introduced to the computer in table form and a table lookup method coupled with linear interpolation was used to find the appropriate values for solution of the growth equations.

Both dry- and wet-growth rates are computed and the lesser of the two rates is chosen as applicable. If the wet rate exceeds the dry rate, all the cloud water encountered by the hailstone is being accreted to it, and the dry-growth regime applies. If the wet rate is less than the dry rate, the heat cannot be dispelled from the stone fast enough to maintain the dry-growth rate and the wet regime applies. Excess water is assumed to be shed from the stone.

The various versions of the feeder cloud model were run on a small-scale digital computer using 20, 30, 40 and 50 μ embryos introduced at 1-km height intervals and time intervals related to the growth rate of the cloud, i.e., 4-min intervals for P25 and R25, and 8-min and 3-min intervals for P12 and P37, respectively.

An arbitrary integration time restriction of 40 min is used in the computer program.

5. Melting of hailstones

The model does not account for melting. In determining whether or not hail reaches the ground, estimates

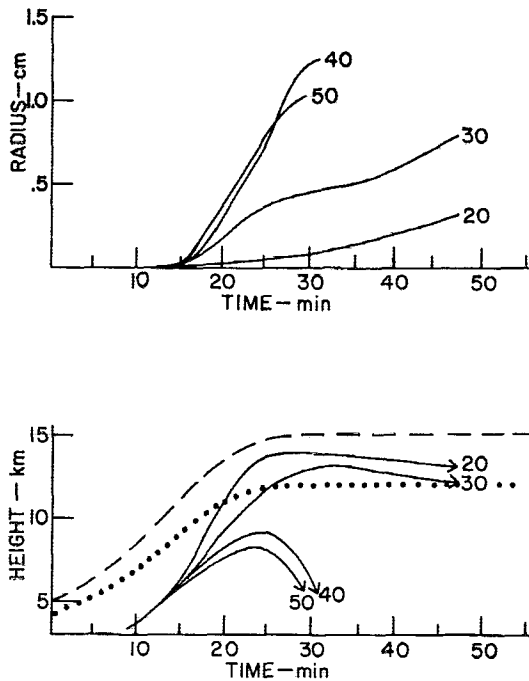


FIG. 4. Sizes and trajectories as a function of time, resulting from 20 to 50 μ embryos introduced at the same point in cloud model P25. Numbers denote initial embryo size. Dashed line refers to cloud top and dotted line indicates updraft maxima.

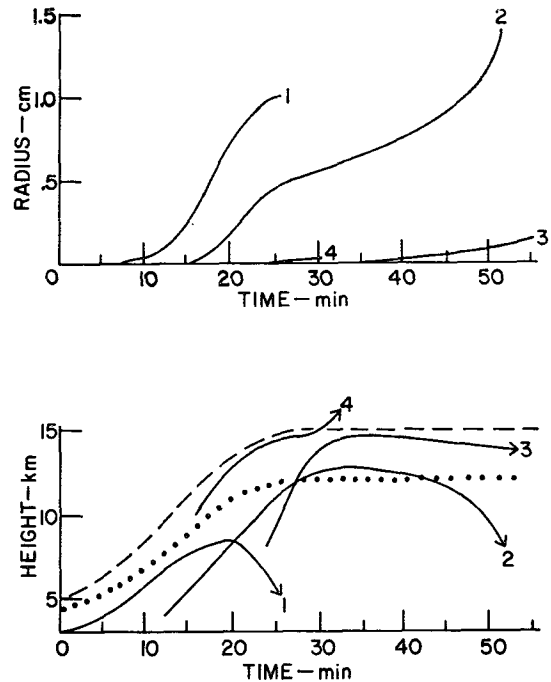


FIG. 5. Sizes and trajectories as a function of time, resulting from a 40 μ embryo introduced at selected points in cloud model P25. Numbers denote trajectory number. Dashed line refers to cloud top and dotted line indicates updraft maxima.

based on size at the melting level and height of that level above the ground (Sulakvelidze *et al.*, 1967) are applied. For the initial conditions used, hailstones must have radii >0.7 cm at the melting level in order to reach the ground.

6. Sample trajectories

As there are so many trajectories available, it would be impractical to present all of them. Instead, sample trajectories are given to illustrate the effects of introducing particles of varying sizes at different times and places in the life of a feeder cloud.

Fig. 4 shows particle sizes and corresponding trajectories that result from the introduction of different sized embryos at the same time and place in P25, i.e., at the base and 8 min into its life. Hailstones growing from 20 and 30 μ embryos rise above the updraft maximum into glaciated regions where growth is slow because of absence of liquid water. The 30 μ embryo results in a somewhat larger particle due to the advantage of being initially larger. Hailstones growing from 40 and 50 μ embryos behave differently. They grow fast enough to fall against the updraft, finally falling through the melting level with radii >1 cm. It is interesting to note that they reach this point in ~ 25 min, a very reasonable time compared with nature.

Another set of sample trajectories (Fig. 5) results from the same size embryo (40 μ) being introduced at different times and places in P25. A 40 μ embryo intro-

duced at the base of the cloud at zero time rolls over and falls from the cloud with a radius near 1 cm. The same size embryo introduced later and slightly higher in the clouds is carried above the updraft maximum. Its growth is quite rapid but slows considerably when it reaches higher regions of the cloud, where liquid water contents are small. However, it eventually gets large enough to fall back through the updraft maximum into liquid water regions of the cloud, where the growth rate increases rapidly. The final size after about 40 min growth is nearing 1.5 cm. Introduction of the embryo later yet and still higher in the cloud (Trajectory 3) results in a rather small hailstone growing very slowly near the top of the cloud. Eventually it would emerge as a fairly large stone if the program was allowed to continue, but these times would be unreasonably long. Trajectory 4 shows the fate of a 40μ embryo that is introduced too near the cloud top and it is shown to be ejected from the updraft region after about 15 min at an extremely small size.

7. Summary of results

It has been shown that the fate of any embryo is dependent upon the time and place of introduction in the cloud and its initial size. It is apparent that the variations in trajectories are tremendous. Nevertheless, the fates of the different embryos fall into a few convenient categories that provide an effective means of summarizing the history of any embryo.

Fig. 6 summarizes the fates of $20\text{--}50 \mu$ embryos introduced at various heights and times in all versions of the feeder cloud model used to date. Considering 20μ embryos growing in P12, it can be seen that embryos introduced early and low fall out as rain without ever freezing. Growth of embryos originating in this region (the "warm-rain" region) is exclusively by coalescence. Embryos introduced much higher in the cloud reach the cloud top, resulting in an area called the "eject" region. Between these extremes lies a hail region, which is further divided into a "cold rain" and a "hail" region.

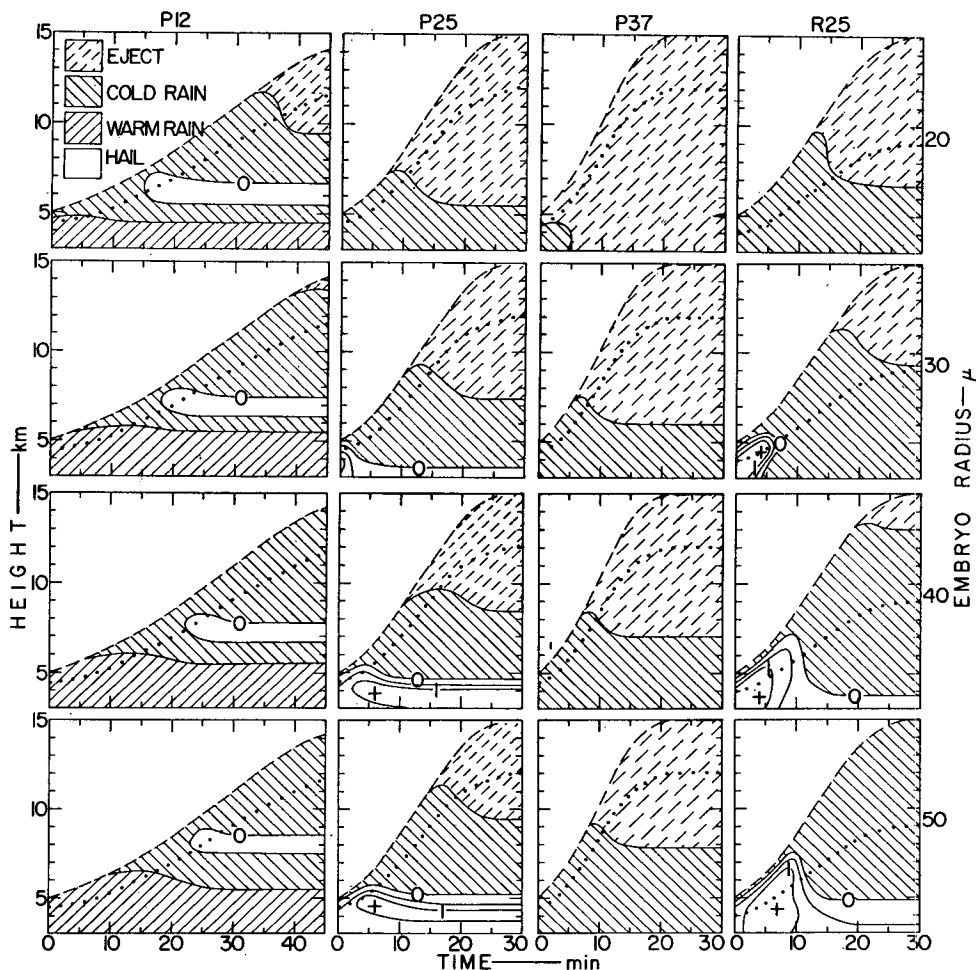


FIG. 6. Fate of $20\text{--}50 \mu$ embryos introduced at various heights and times in all versions of the feeder cloud model. Dashed lines refer to cloud top and dotted lines indicate updraft maxima in each version of the model. Plus signs denote approximate points where introduction of a given embryo yielded the largest hail in P25 and R25.

The cold-rain region results from embryos that fall out as hailstones <0.7 cm or fail to reach 0.7 cm radius within the 40-min time restriction, and therefore are assumed to melt prior to reaching the ground. As shown in Fig. 6, the cold-rain region straddles the hail region. It is therefore convenient to refer to an upper and lower cold rain region. As discussed in Sections 4 and 5, embryos which reach a size >0.7 cm in 40 min or less outline the hail region.

a. Effects of changes in updraft magnitude and embryo size

A comparison of the P-versions of the model (Fig. 6) shows the effects of changes in updraft magnitude and embryo size in the feeder cloud model. As the updrafts increase in strength, the regions move downward in the cloud. With increasing embryo size, all regions progress upward in the cloud, but this effect appears less pronounced.

The warm rain disappears for all embryo sizes in going from P12 to P25.

The hail region is below the cloud base for $20\ \mu$ embryos in P25 and for all embryos up to $50\ \mu$ in P37. Even though no hail reaches the ground in P37 (in this model), it cannot be concluded that hail and strong updrafts are not related. One must consider the possible occurrence of greater than adiabatic liquid water contents and larger embryos than we have considered so far.

Since the boundaries between the various regions show little variations with time, it can be said that the P-versions are not very time-dependent, except very early in the life of the cloud.

Hailstone radii range between 0 and 1.3 cm, with the largest stones being produced in P25. It is possible that some other version of the model not studied here, say P30, would produce larger hail. Forty and $50\ \mu$ embryos introduced after ~ 3 min in P25 generally define a region of hail exceeding 1 cm, with embryos released near 4.5 km between 5–10 min yielding the largest hail. The area outlining hailstones >1 cm is smaller for $50\ \mu$ embryos and does not include embryos introduced at the base, as is the case with $40\ \mu$ embryos. This suggests that an optimum embryo exists that will produce the largest amount of big hail for any given set of conditions in the cloud.

There are prominent cold-rain regions in all P-versions of the model, indicating much small hail aloft in the clouds. As the updraft magnitudes increase, the lower cold-rain region gradually moves out of the cloud at the base. Except for $20\ \mu$ embryos introduced in P37, the size of the cold-rain region does not change much.

b. Effects of updraft profile shape

An idea of the effects related to shape of the updraft profile can be made by comparing P25 and R25 in Fig. 6. Certain similarities exist in that no hail regions evolve using $20\ \mu$ embryos, the hail regions get progressively larger as the embryo size increases, and the hailstone

sizes achieved are approximately the same in either version.

In the hail regions R25 appears to be much more responsive to the time that the embryo is introduced, as evidenced by the peaks early in the life of the cloud. All particles resulting from embryos introduced in the R25 hail regions achieve a good share of their growth above the updraft maximum and eventually become large enough to fall back through the maximum, whereas in P25 the major growth was below the updraft maximum. Embryos introduced early in R25 find themselves in relatively weaker updrafts above the maximum but still in the region of quite high liquid water content where growth is rapid. Embryos introduced after ~ 12 min are also carried above the updraft maximum, but by the time this level is reached, most of the cloud water is frozen, so that the resulting hailstones are smaller than those grown from embryos introduced earlier. After 12 min, time of introduction loses its importance in R25, since the model is approaching a steady-state condition. In P25 this was not so pronounced and occurred much earlier in the life of the cloud.

The largest hail in R25 results from embryos introduced early and slightly above the cloud base. The axis of maximum hailstone size increases with height and time of introduction of 30 – $50\ \mu$ embryos, while the axis is oriented essentially horizontal in P25. Thus, the combination of height and time of embryo introduction seems to be more important if the updraft maximum is lower in the cloud. The maximum size observed (~ 1.3 cm) appears to be independent of initial embryo size, at least in the 30 – $50\ \mu$ embryo range.

The area of the eject region decreases faster in R25 than in P25 as embryo size increases and is nonexistent for $50\ \mu$ embryos. Consequently, the cold-rain regions are larger in R25 than in P25.

c. Mass convergence zone³

There is some indication of a mass convergence zone when the updraft maximum is lower in the cloud. Fig. 7 shows the trajectories of $40\ \mu$ embryos introduced into the hail regions of R25. Particles introduced in the first 8 min converge above the updraft maximum between 9–10 km at about 16–20 min. They are restricted to an even smaller zone when particles introduced within the first 4 min of the cloud's life (hatched region) are considered. The vertical thickness of the zone is less than 0.5 km during the time period of approximately 13–19 min. This phenomenon is not observed when embryos are introduced after R25 begins to approach steady-state conditions and barely at all in P25. For embryos released early, R25 tends to act like the Russian hailstorm model (Sulakvelidze *et al.*), where an accumulation zone forms above the maximum in vertical velocity.

³ Some authors refer to this region as an accumulation zone.

The shape of the updraft profile obviously plays an important role in the evolution of a storm. If the updraft maximum is low in the cloud, embryos can grow in a region of high liquid water content and an accumulation zone develops. This suggests a pulsating storm, in which the sheer weight of the water and ice would eventually destroy the updraft. An updraft maximum high in the cloud appears more conducive to the development of a steady-state system with the major hailstone growth below the updraft maximum.

The comments in the preceding paragraph must be considered speculation because hailstorms are extremely complex and this model does not include depletion or addition of rainwater, so that any feedback mechanisms that might exist between particles starting at different times and places in the cloud are not accounted for.

8. Conclusions and future plans

Hail is formed readily in the model for updraft maxima ranging from 12 to greater than 25 m sec⁻¹, with no further assumptions other than the existence of adiabatic cloud water contents and some embryos in the lower part of the feeder cloud.

Storm rotation, sloping updraft and strong wind shear, although sometimes observed in severe hailstorms, are not essential items in hailstone formation. Hail is a perfectly natural form of precipitation, the

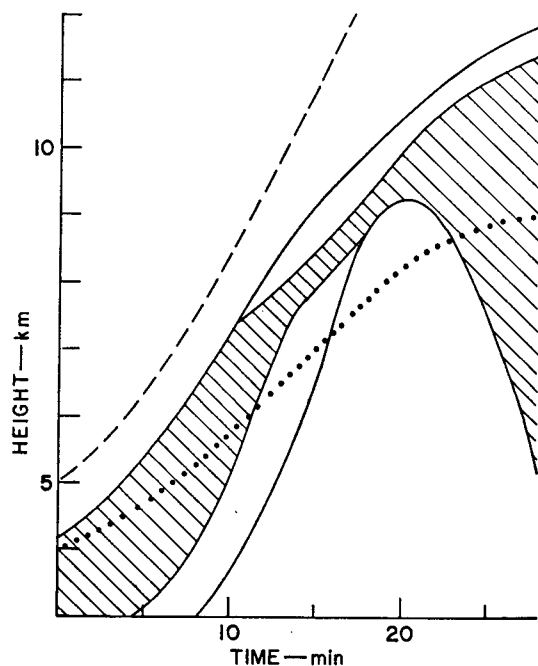


FIG. 7. Envelope containing all trajectories resulting from introduction of 40 μ embryos in cloud model R25. Solid curves outline the envelope of trajectories from embryos introduced in the first 8 min and the hatched area corresponds to embryos introduced in the first 4 min of the model's life. Dashed line refers to cloud top and dotted line indicates updraft maxima.

general conditions for its formation being present almost every day in many areas of the world.

The feeder cloud model describes quite well many of the hailstorms that occur in the northern Great Plains.

Future plans for the feeder cloud model include the following: 1) studying the effects of allowing a film of water of some thickness to accumulate on the hailstone during wet growth rather than assuming all excess liquid to be shed; 2) studying the effects of freezing the liquid cloud water at various temperatures and rates; and 3) studying the effects of adding superadiabatic liquid water contents.

Acknowledgments. The author wishes to thank Dr. Arnett S. Dennis for his many helpful comments and suggestions throughout the course of this study and during the preparation of this paper. The research was supported by the Atmospheric Sciences Section, National Science Foundation, under NSF Grant GA-935.

APPENDIX

Development of Hailstone Growth Equations

1. Equation for dry-growth rate

The changes in mass M per unit time of a growing hailstone can be expressed as the sum of the mass changes due to collection of supercooled cloud droplets and the collection of ice crystals. This can be written as

$$\frac{dM}{dt} = \frac{dM_l}{dt} + \frac{dM_s}{dt}, \quad (\text{A1})$$

where the subscripts, l and s , refer to the liquid and solid masses, respectively. This expression accounts for the presence of liquid droplets and ice crystals separately, or for their simultaneous existence. The coexistence of ice and liquid is apparently a quite common occurrence in convective clouds (e.g., Vali, 1968) and should be a consideration in the development of hailstone growth equations.

In terms of heat balance, when dry-growth conditions are assumed to exist, it follows that the heat transferred to the hailstone through the release of latent heat of fusion and sensible heat transfer in the freezing process is less than the heat that can be transferred back to the surroundings. Therefore, the change in mass per unit time due to collection of liquid droplets can be written as

$$\frac{dM_l}{dt} = \pi R^2 V_i X_l E_l, \quad (\text{A2})$$

and for collection of ice crystals by

$$\frac{dM_s}{dt} = \pi R^2 V_i X_s E_s, \quad (\text{A3})$$

where $\pi R^2 V_t$ is the volume of a cylinder swept out by a hailstone falling at terminal velocity V_t , X the mass of the particles encountered (expressed as liquid water content gm m^{-3}), and E the collection efficiency.

If spherical particles are assumed, then the mass of the particles in the volume can be given by

$$M = \frac{4\pi R^3 \rho_e}{3}, \tag{A4}$$

where R is the radius (cm), and ρ_e the density of the particles (gm cm^{-3}). Then

$$\frac{dM}{dt} = 4\pi R^2 \rho_e \frac{dR}{dt}. \tag{A5}$$

Making the appropriate substitutions for dM/dt , dM_i/dt , and dM_s/dt in (A1) and solving for dR/dt , we get the equation for dry growth,

$$\frac{dR}{dt} = \frac{V_t X_i E_i}{4\rho_e} + \frac{V_t X_s E_s}{4\rho_e}. \tag{A6}$$

2. Equation for wet-growth rate

The dry-growth state continues as long as the hailstone is able to dispel all the heat resulting from collisions with liquid droplets while maintaining a temperature $< 0\text{C}$. However, as increasing amounts of liquid water are encountered, the temperature of the stone gradually rises. Finally, as the temperature of the surface of the stone reaches 0C , a thin film of water forms on the stone and the condition of wet growth has been reached. Hailstone growth under these conditions depends primarily on the rate at which heat can be transferred away from the stone to the environment.

It is assumed that any excess liquid is shed from the stone and plays no part in the physics of hailstone growth (Ludlam, 1958), despite the findings of List (1963) which showed that some liquid became trapped in a lattice structure forming in the stone.

The rate at which a wet hailstone is able to transfer heat to its surroundings is $4\pi R a (-KT + LD\Delta\rho_w)$, where the first term in the parentheses refers to heat conduction away from the stone and the second to evaporative cooling. In addition, T is the temperature of the liquid droplets and cloud air ($^{\circ}\text{C}$), a the ventilation coefficient (dimensionless), K the thermal conductivity of cloud air [$\text{cal gm}^{-1} \text{sec}^{-1} (^{\circ}\text{C})^{-1}$], L the latent heat of vaporization ($597.3 \text{ cal gm}^{-1}$), D the diffusivity of water vapor ($\text{cm}^2 \text{sec}^{-1}$), and $\Delta\rho_w$ the saturation vapor density at the temperature of the hailstone minus that at the temperature of the cloud air (gm cm^{-3}). The heat that must be dissipated per gram of accreted cloud water is $(L_f + C_w T)$, where L_f is the latent heat of fusion (79.7 cal gm^{-1}), and C_w the specific heat of liquid water [1.0 cal gm^{-1} ($^{\circ}\text{C}$) $^{-1}$]. Therefore,

gm^{-1} ($^{\circ}\text{C}$) $^{-1}$]. Therefore,

$$\frac{dM_i}{dt} = \frac{4\pi R a (-KT + LD\Delta\rho_w)}{L_f + C_w T}. \tag{A7}$$

It should be noted that the temperature in (A7) should actually be treated as a difference between hailstone and cloud air; however, since the hailstone is assumed to be at 0C , only the cloud temperature need be considered.

Next, if liquid and ice exist simultaneously, it is necessary to consider the sensible heat transfer resulting from collisions with ice crystals. Since the crystals will be colder than the stone, the net effect is to cool the hailstone, with a resultant increase in its mass. In other words, a portion of the excess heat contained by the hailstone can be taken up by the cooler ice crystals, so that some additional growth is obtained. The change in mass due to the combination of ice and water can be expressed by

$$\frac{dM_i}{dt} = \frac{4\pi R a (-KT + LD\Delta\rho_w) - \frac{dM_s}{dt} C_i T}{L_f + C_w T}, \tag{A8}$$

where C_i is the specific heat of ice and is given as $0.5 \text{ cal gm}^{-1} (^{\circ}\text{C})^{-1}$.

The change in M_s due to the interception of ice crystals yields the same expression as given in (A3), except E_s , the collection efficiency, will be much greater than in dry growth, because of the ability of the liquid surface of the stone to rapidly collect any ice crystals that are encountered. In wet-growth conditions, E_s is assumed to be unity or 100%.

Substituting for dM_i/dt in (A1) and rearranging, we obtain

$$\frac{dM}{dt} = \frac{4\pi R a (-KT + LD\Delta\rho_w)}{L_f + C_w T} + \frac{dM_s}{dt} \left(1 - \frac{C_i T}{L_f + C_w T} \right). \tag{A9}$$

Substituting for dM_s/dt and dM from (A3) and (A5) and solving for dR/dt , we have the equation for wet growth,

$$\frac{dR}{dt} = \left(\frac{1}{L_f + C_w T} \right) \left(\frac{a}{R\rho_e} \right) (-KT + LD\Delta\rho_w) + \frac{V_t X_s E_s}{4\rho_e} \left(1 - \frac{C_i T}{L_f + C_w T} \right). \tag{A10}$$

The ventilation coefficient can be calculated from

$$a = 1 + 0.22F\sqrt{\text{Re}}, \tag{A11}$$

where Re is the Reynolds number and F is the Frossling

number, which is a function of Re . The expression in (A11) was determined by experiments by Kinzer and Gunn (1951). They found that for $Re \leq 1$, $F=0$, then rising to a maximum of 2.2 for $1 < Re \leq 2.1$. For $2.1 < Re \leq 100$, F falls off again, gradually approaching unity, a value at which it remains when $Re > 100$ (Byers, 1965, p. 113).

The Reynolds number can be calculated from

$$Re = \frac{2RV_t \rho_a}{\eta}, \quad (A12)$$

where ρ_a is the density of the cloud air (gm cm^{-3}), and η the viscosity of the air ($1 \text{ gm cm}^{-1} \text{ sec}^{-1} = 1 \text{ poise}$).

The density can be found from the equation of state,

$$\rho_a = \frac{P}{R_a T_v}, \quad (A13)$$

where $R_a = 2.87 \times 10^6 \text{ ergs gm}^{-1} (\text{°K})^{-1}$ (gas constant for dry air), T_v is the virtual temperature in °K , and P the pressure in dynes cm^{-2} .

The viscosity of the air can be represented by an analytic expression based on Table 113 of the *Smithsonian Tables* as

$$\eta = (1.718 + 0.0052T)10^{-4}. \quad (A14)$$

An expression for diffusivity is given in the *Smithsonian Tables* as

$$D = D_0 \left(\frac{T}{T_0} \right)^n \frac{P_0}{P}, \quad (A15)$$

where P is pressure in millibars and the subscript zero denotes conditions at some reference point, in this case taken to be 1000 mb and 273.2K. The exponent n is an empirical constant given as 1.81. This expression is slightly different from that used by Ludlam (1958), but yields essentially the same results.

The conductivity can be given by an analytic expression developed from data in the *Smithsonian Tables* as

$$K = (5.8 + 0.0184T)10^{-5}. \quad (A16)$$

REFERENCES

- Atlas, D., 1966: The balance level in convective storms. *J. Atmos. Sci.*, **23**, 635-651.
- Battán, L. J., and C. H. Reitan, 1957: Droplet size measurements in convective clouds. *Artificial Stimulation of Rain*, New York, Pergamon Press, 184-191.
- Byers, H. R., 1965: *Elements of Cloud Physics*. The University of Chicago Press, 191 pp.
- Das, P., 1962: Influence of wind shear on the growth of hail. *J. Atmos. Sci.*, **19**, 407-414.
- Davis, L., P. Willis and O. Rhea, 1969: Observational and numerical studies of updraft structure. Hailstorm Models Project, Vol. III, Rept. 69-1, NSF Grant GA-935, South Dakota School of Mines and Technology, Rapid City, 59 pp.
- Dennis, A. S., C. A. Schock and A. Koscielski, 1970: Characteristics of hailstorms of western South Dakota. *J. Appl. Meteor.*, **9**, 127-135.
- Donaldson, R. H., 1961: Radar reflectivity profiles in thunderstorms. *J. Appl. Meteor.*, **18**, 292-305.
- Douglas, R. H., 1963: Recent hail research: A review. *Meteor. Monogr.*, **5**, No. 27, 157-167.
- Draginis, M., 1958: Liquid water content within the convective clouds. *J. Meteor.*, **15**, 481-485.
- Gunn, R., and G. D. Kinzer, 1949: The terminal velocity of fall for water droplets in stagnant air. *J. Meteor.*, **6**, 242-248.
- Hirsch, J. H., and C. L. Schock, 1968: Cumulus cloud characteristics over western South Dakota. *J. Appl. Meteor.*, **7**, 882-885.
- Hitschfeld, W., and R. H. Douglas, 1961: A theory of hail growth. Alberta Hail Studies, Sci. Rept. MW-35, Montreal, McGill University, 19-29.
- Humphreys, W. J., 1940: *Physics of the Air*. New York, McGraw-Hill, p. 359.
- Kinzer, G. D., and R. Gunn, 1951: The evaporation, temperature, and thermal relaxation-time of freely falling waterdrops. *J. Meteor.*, **8**, 71-83.
- Kopcewicz, T., 1965: Selected problems in hail physics and hail suppression. *Przeł. Geofiz.*, Warsaw University, **10**, 84 pp.
- List, R., 1963: General heat and mass exchange of spherical hailstones. *J. Atmos. Sci.*, **20**, 189-197.
- , 1958: *Smithsonian Meteorological Tables*. Washington, D. C., Smithsonian Institute, 527 pp.
- Ludlam, F. H., 1958: The hail problem. *Nubila*, **1**, No. 1, 1-96.
- , 1959: Hailstorm studies, 1958. *Nubila*, **2**, No. 1, 7-27.
- MacCready, P. B., Jr., and D. M. Takeuchi, 1968: Precipitation initiation mechanisms and droplet characteristics of some convective cloud cores. *J. Appl. Meteor.*, **7**, 591-602.
- Macklin, W. C., and F. H. Ludlam, 1961: The fallspeeds of hailstones. *Quart. J. Roy. Meteor. Soc.*, **87**, 72-81.
- Rosinski, J., and T. R. Kerrigan, 1969: The role of aerosol particles in the formation of rain drops and hailstones in severe thunderstorms. *J. Atmos. Sci.*, **26**, 695-715.
- Saunders, C. P. R., 1968: The influence of cloud electrification on ice crystal aggregation. *Proc. Intern. Conf. Cloud Physics*, Toronto, 619-623.
- Scorer, R. S., 1958: *Natural Aerodynamics*. New York, Macmillan, 312 pp.
- Sulakvelidze, D. K., N. Sh. Bibilashvili and V. F. Lapcheva, 1967: Formation of precipitation and modification of hail processes. Israel Program for Scientific Translations, Jerusalem, Israel, 208 pp.
- Vali, G., 1968: Ice nucleation relevant to formation of hail. Sci. Rept. MW-58, Montreal, McGill University, 51 pp.
- , and E. J. Stansbury, 1965: Time-dependent characteristics of the heterogeneous nucleation of ice. Sci. Rept. MW-41, Montreal, McGill University, 31 pp.
- Vittori, O., and G. D. Caporriacco, 1959: The density of hailstones. *Nubila*, **2**, No. 1, 51-57.
- Warner, J., 1955: The water content of cumuliform cloud. *Tellus*, **7**, 449-457.
- Weickmann, H. K., and H. J. aufm Kampe, 1953: Physical properties of cumulus clouds. *J. Meteor.*, **10**, 204-211.
- Weinstein, A. I., and L. G. Davis, 1968: A parameterized numerical model of cumulus convection. Rept. No. 11, NSF GA-777, Dept. of Meteorology, Pennsylvania State University, 43 pp.